AD-A080 708 CALIFORNIA INST OF TECH PASADENA DIV OF CHEMISTRY A--ETC F/G 7/4
A 13C NMR STUDY OF THE ADSORBED STATES OF CO ON RH DISPERSED ON--ETC(U)
JAN 80 T M DUNCAN, J T YATES, R W VAUGHAN N00014-75-C-0960
UNCLASSIFIED TR-15 NL

END
DATE FILMED
3-80
DDC

(15) N00014-75-C-0960 OFFICE OF NAVAL RESEARCH
Contracts N00014-77-F0008 and N00014-75-C960

(6) (9) Technical Report #15

A ^{13}C NMR Study of the Adsorbed States of CO on Rh Dispersed on Al_2O_3.

(10) T. M./Duncan, J. T./Yates, Jr., R. W./Vaughan

Division of Chemistry and Chemical Engineering
California Institute of Technology
Pasadena, California 91125

(14) TR-15

(11) Jan 80 (12) 42

To be published in the J. Chem. Physics

A ^{13}C NMR STUDY OF THE ADSORBED STATES OF CO ON Rh DISPERSED ON Al_2O_3[#]

T.M. DUNCAN, J.T. YATES, JR.[*], AND R.W. VAUGHAN[**]

Division of Chemistry and Chemical Engineering
California Institute of Technology
Pasadena, California 91125

January 1980

PACS Numbers: 82.65.Jv, 82.80.Di, 76.60.Cq, 76.60.Es

[#] Supported in part by the Office of Naval Research under Contracts N00014-75-C-0960 and N00014-77-F-0008

[*] Work performed while a Sherman Fairchild Distinguished Scholar at Caltech. Permanent address: Surface Science Division, National Bureau of Standards, Washington, D.C. 20234

[**] Deceased

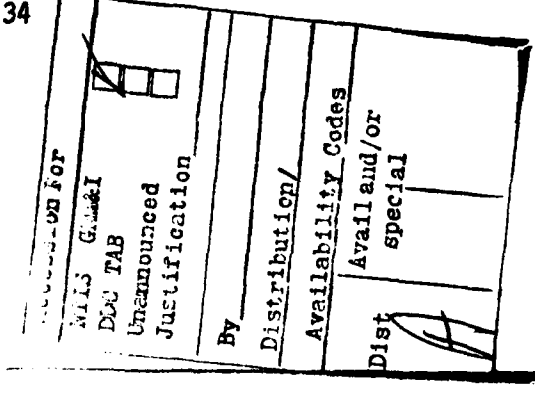

ABSTRACT

The results of nuclear magnetic resonance (NMR) spectroscopy have been analyzed with respect to previous infrared studies of CO adsorbed on Rh dispersed on Al_2O_3 to quantify the site distribution and to describe the adsorbed state. The ^{13}C NMR spectra account for all the ^{13}CO adsorbed on a 2.2% Rh on Al_2O_3 substrate. Although the spectra from the different adsorbed states of CO overlap, the lineshapes may be separated into two components based on differences in the ^{13}C spin-lattice relaxation times. These two components have been assigned to the ^{13}CO dicarbonyl formed on single Rh atoms and to ^{13}CO adsorbed on Rh rafts. The component attributed to the CO adsorbed on the raft sites is further separated into linear and bridged CO state contributions based on chemical shift information, yielding a quantitative distribution of the three adsorbed states of CO on Rh. The ^{13}CO distribution is used to estimate the molar integrated intensities of the infrared spectrum of ^{13}CO on Rh at high coverage and to determine the degree of dispersion of Rh on the Al_2O_3. The ^{13}C NMR lineshapes of CO adsorbed on Rh are different from the powder pattern of $Rh_2Cl_2(CO)_4$. The lineshape of the dicarbonyl surface specie is narrowed to a Lorentzian curve by reorientation at the site and the lineshape of CO on the Rh rafts is modulated by exchange between sites on a single raft. The ^{13}C relaxation time distribution provides further evidence for the existence of isolated Rh atoms on the Al_2O_3 surface.

I. INTRODUCTION

The adsorption of molecules on transition metals dispersed on oxide suppor has been studied extensively by transmission infrared spectroscopy (1,2). More recently, inelastic electron tunneling spectroscopy has improved the sensitivit and extended the spectral range of the vibrational studies (3). High resolutio solid state nuclear magnetic resonance (NMR) spectroscopy (4-6) has been applie to the study of molecules adsorbed on high area surfaces (7,8). NMR spectra ar sensitive to molecular motions on the order of the linewidth, which is typicall 10 to 10^4 Hz for chemisorbed molecules. Motions such as surface diffusion or hindered rotation are usually in this frequency range. Since the integrated intensity of the NMR spectrum is linearly proportional to the concentration, it is possible to calculate absolute site populations. The synergistic combinatio of vibrational and NMR spectroscopies provides a unique tool for the characteriz of the nature of the adsorbed molecule. The ^{13}C NMR study of CO adsorbed on supported Rh has only recently been reported (9) and represents the first example of the use of this technique to study chemisorption on dispersed metals Such systems are difficult to study mainly because the dilute spins yield an extremely weak resonance signal. We report here a more detailed ^{13}C NMR study of the adsorbed states of CO on Rh dispersed on Al_2O_3.

In dilute ^{13}C spin systems, the homonuclear dipolar broadening is weak; thus, the major effects observed in the NMR spectra are the chemical shift interaction and the heteronuclear broadening. Two features of the chemical shift interaction are most useful in characterizing the ^{13}C electronic environment. The average resonant frequency, or the center of mass, of the lineshape can be compared with the chemical shifts of known compounds for identification in a fingerprinting fashion. The center of mass of a specie is independent of the motional properties of the molecule; thus, the broad line of a solid has

the same center of mass as a rapidly reorienting liquid, provided there are no chemical changes in the phase transition. Second, the principal components of the second rank chemical shift tensor are good indicators of the molecular symmetry and the degree of anisotropy of the electron distribution. Various molecular motions, such as wagging, rotation, or diffusion, will uniquely modulate the rigid chemical shift powder pattern. Although there exist reasonable calculations to predict trends in isotropic chemical shifts within a group, such as alkanes, alkenes, or carbonyls, there is at present no general theory to cover the entire range of carbon compounds (10-12). Thus, to date the chemical shift data has been analyzed in a correlative fashion. To investigate the nature of an unknown surface specie, it is necessary to study the chemical shift powder pattern of a number of related, well-defined compounds. In addition, the specific modulation of the characteristic chemical shift tensor by molecular reorientation provides information on the frequency and the nature of the motion (5). The major heteronuclear dipolar interactions for the ^{13}C nuclei in the Rh on Al_2O_3 system are with the ^{27}Al of the support, the ^{1}H of the hydroxyls and adsorbed water, and the ^{103}Rh. However, because of large internuclear distances between ^{13}C and ^{27}Al or ^{1}H and the low gyromagnetic ratio of ^{103}Rh, each of these interactions is predicted to be much less than the chemical shift anisotropy.

The spin-lattice relaxation time, T_1, of surface adsorbed molecules may also be used to characterize the local environment on the substrate (7,8). In general, the relaxation is determined by local magnetic fields fluctuating at rates near the Larmor frequency of the nucleus of interest. Thus, the T_1 of the nucleus of interest is affected by dipolar interactions with neighboring unpaired electrons or other nuclei with magnetic moments, exchange between adsorption sites with different anisotropic shieldings, or librations through

chemical shift orientational anisotropy. Under certain conditions (8), a measurement of the T_1 as a function of temperature can be used to determine the correlation time for molecular reorientation or diffusion, average internuclear distances, and the heterogeneity of the distribution of adsorption sites on the surface, i.e., isolated or clustered. In some dilute spin systems, less than ~10^{20} spins/cm^3, there may exist a nonuniform distribution of T_1's, resulting from an angular distribution of axes of reorientation or local concentration of adsorbates and paramagnetic centers. In these cases, it may be possible to use the T_1 distribution to differentiate between dissimilar adsorbed species.

The adsorption of CO on Rh dispersed on Al_2O_3 has been studied extensively by infrared spectroscopy (13-17) combined with electron microscopy (18), and by inelastic electron tunneling spectroscopy (19). The infrared results were reviewed briefly in previous papers (14,15). The three generally accepted states of CO on Rh dispersed on Al_2O_3, originally proposed by Yang and Garland (13), are a dicarbonyl site (specie I), a linearly bonded CO (specie II), and a multi-bonded bridging CO (specie III).

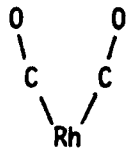

I

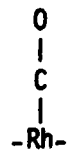

II

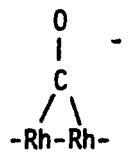

III

Species II and III are believed to form on Rh atoms congregated into small rafts or islands on the Al_2O_3 support (13,14,17,18). There is some controversy as to the

nature of specie I. It is maintained by some workers (18) that the dicarbonyl specie forms on the edge atoms of Rh rafts, while others (13,14,17) suggest that these Rh sites exist as isolated atoms on the surface. This topic will be addressed later in this work. It has been found that the rate of isotopic exchange (15) and the chemical reactivity and selectivity of the Rh responsible for sites II and III are different from the Rh in specie I (16,20,21). Thus, it would be useful to know the absolute populations of the two states.

II. EXPERIMENTAL PROCEDURES

The samples of Rh dispersed on Al_2O_3 were treated and analyzed in a combined infrared/NMR cell. The infrared cell, a stainless steel body with single-crystal CaF_2 windows, as well as the all-metal 10^{-8} Torr vacuum system have been described previously (14). The infrared cell was modified to accommodate NMR samples by welding a ¼ in. I.D. stainless steel fitting to a port drilled in a central section of the cell. The NMR sample tubes attached to this port consist of a stainless steel Cajon VCR fitting welded to a copper tube fused to 10 mm O.D. pyrex glass. The NMR tube may be permanently detached from the cell by pinching off the copper section to form an ultrahigh-vacuum cold-welded seal. This separation does not perturb the vacuum integrity in either section. The total dead volume of the cell is ~50 cm^3.

The infrared scans were recorded in the absorbance mode on a Perkin-Elmer 180 grating spectrometer operated in the double beam option. Calibration procedures using CO(g) and H_2CO(g) were described previously (14). The spectral resolution in the 2000 cm^{-1} region was set at 2.6 cm^{-1}.

The NMR spectra were taken on a 1.32 Tesla spectrometer described previously (22), stabilized with an external pulsed lock system to drifts of less than

1 ppm over an 8-hour period. The single resonance probe is tuned to 14.175 MHz with a 10 mm I.D., 14 mm long coil. The coil is enclosed in a glass dewar, and the sample temperature is lowered by drawing LN_2 past the coil with a small roughing pump. The NMR spectra were obtained by Fourier tranforming the free induction decay after a 90^o pulse. A 180^o prepulse was applied at time τ before the 90^o pulse to every other decay, and the transients were alternately added and subtracted to eliminate instrumental artifacts. Also, the longitudinal relaxation time, T_1, of the sample may be determined by the intensity of the magnetization as a function of τ (23). The field strengths for the 90^o and 180^o pulses are 78 and 70 gauss, or 84 and 75 KHz for ^{13}C nuclei, respectively, sufficient to satisfy the criterion for nonselective pulses (24). The ^{13}C NMR spectra of the adsorbed CO reported here are the accumulation of at least 400 000 averages at 300 K and 100 000 at 80 K. The chemical shift scale was calibrated by the ^{13}C resonance in tetramethylsilane (TMS, 0 ppm), adamantane (-34.4 ppm) (10) and sodium formate dissolved in water (-168.7 ppm). Note that all features are reported on the σ scale for chemical shifts relative to TMS (5). The ^{13}C spin counts were calibrated at 300 K with natural abundance ^{13}C adamantane and at 80 K with 70% ^{13}C-enriched barium carbonate. With the number of averages taken, the error limits of the NMR spectra are ±2% of the ^{13}C spin count and ±7 ppm (one channel) on the frequency scale.

The 2.2% by weight Rh on Al_2O_3 substrate was prepared as described previously (14). Briefly, $RhCl_3 \cdot 3H_2O$ is dissolved in a water: acetone (1:10) suspension of Al_2O_3 and then sprayed onto a CaF_2 window and simultaneously onto a pyrex glass plate, both at 355 K. The CaF_2 window, covered with ~11 mg/cm^2 of sample, is mounted in the infrared cell. The deposit on the pyrex plate is scraped off and tamped into the bottom of the NMR tube. The NMR sample is ~0.50 g (5.9×10^{19} Rh atoms) with a void fraction of 75%, calculated from the bulk Al_2O_3 density. The cell is assembled and both the

infrared and NMR samples are outgassed, heated to 425 K at 15 K/hr, and reduced in H_2 as before (14). For each of the three charges of H_2 (Matheson grade 99.9995% pure) to the sample, the ratio of H_2 to Rh was ~100:1. The Al_2O_3-supported Rh substrate is outgassed at 450 K for 12 hours to a background pressure of $\sim 10^{-6}$ Torr, then slowly cooled (25 K/hr) to room temperature. A background infrared scan from 4000 to 1200 cm^{-1} is taken to assure that the sample is free of impurities observable by IR. The typical H/Rh ratio measured on freshly prepared substrates at 300 K was 0.90.

The Al_2O_3, "Alon-C," was prepared by Cabot, Inc., Boston, Massachusetts. The powder has a specific surface area of 90 m^2/g and contains 0.21 ± 0.01 % Fe and 0.38 ± 0.05% Cl by weight, as determined by atomic absorption and selective ion electrode analysis, respectively. The Al_2O_3 was commercially prepared by fuming $AlCl_3$ in a hydrogen/oxygen flame at ~2100 K; thus, one would expect that the Fe is incorporated into the Al_2O_3 framework during the oxidation by substituting for Al atoms. The electron paramagnetic spectrum of the Alon-C powder at 8 K and the microwave frequency at 9.25 GHz shows a sharp transition at g = 4.25. Thus, the iron is atomically dispersed throughout the sample and is not clustered in small particles. Also, the g value is typical of Fe^{++} in oxides, rather than Fe^{+++} which has a g value of 2.0 at levels of 0.02% in natural sapphire (Al_2O_3) (25). After reduction and outgassing, the Al_2O_3-supported Rh samples contained 1.36 to 1.56% Cl by weight. Thus, 48 to 57% of the Cl introduced as $RhCl_3 \cdot 3H_2O$ was retained by the sample. The HCl formed during the reduction of $RhCl_3 \cdot 3H_2O$ is most likely reacting with the Al_2O_3 surface. At room temperature, HCl reacts with Al_2O_3 to produce new hydroxyl groups and H_2O, as observed by infrared studies (26). The HCl is chemisorbed by inserting into an Al-O-Al bond to form Al-Cl and Al-OH or by exchanging with an Al-OH site to form Al-Cl and H_2O.

The ^{13}CO (90% enriched) obtained from Merck Isotopes and spectroscopic grade CO, both in glass breakseal bulbs, were used without further purification. The $Rh_2Cl_2(CO)_4$, prepared by Alfa-Ventron, was enriched to ~20% ^{13}C in an all-g closed vessel by exposing the crystals to $^{13}CO(g)$ for 7 days at 370 K, which is below the decomposition temperature (27).

III. RESULTS

A. ^{13}C NMR Spectrum of $Rh_2Cl_2(CO)_4$

The ^{13}C T_1 of $Rh_2Cl_2(CO)_4$ is ~30 minutes at 300 K, which prohibited extended averaging. The sum of 328 transients taken once every 45 minutes is shown in Figure 1. The center of mass, or average spectral frequency, of the spectrum is -186 ± 7 ppm, in close agreement with the observed isotropic chemica shift of the compound in solution, -180.4 ppm (28). The lineshape is fit with a nonlinear least-squares theoretical chemical shift powder pattern, convoluted with a Lorentzian broadening function (29). The principal components of the computed fit are σ_{11} = 99 ppm, σ_{22} = -299 ppm, and σ_{33} = -306 ppm, yielding an isotropic chemical shift of -169 ppm. The discrepancy between the isotropic value of the fit and the computed center of the line indicates that the data are not a fully developed powder pattern. The most probable cause is that the spin-lattice relaxation process, which is principally the result of librations through different chemical shift shieldings, has a pronounced angular dependence as observed in other transition metal carbonyls (30,31). Thus, portions of the spectrum have relatively longer T_1's, resulting in a lower intensity at these orientations and causing a slightly distorted pattern.

B. ^{13}C NMR Spectrum of ^{13}C Adsorbed on Rh

A 2.2% Rh on Al_2O_3 substrate was exposed to ~50 Torr of ^{13}CO at 300 K. The integrated intensities of the infrared spectrum, calibrated against the

CO uptake of previous samples (14), indicate that the ratio of adsorbed CO to Rh is ~0.9. The integrated intensity of the NMR spectrum, shown in Figure 2(a), yields a CO-to-Rh ratio of 0.87 ± 0.02. When the sample is cooled to 80 K, after pumping out the excess CO(g) to 0.02 Torr to prevent the formation of any physisorbed CO at low temperatures, the NMR spectrum broadens, as illustrated in Figure 2(b), but the temperature-compensated integrated intensity remains constant. The center of mass of the ^{13}C NMR spectrum is constant with temperature change, at -191 ± 7 ppm.

When the pressure of the ^{13}CO is reduced from 50 Torr to 10^{-6} Torr, the ^{13}C NMR lineshape intensity at 300 K decreased uniformly by 15%, with no change in the linewidth or the center of mass. A sample of Al_2O_3, with no Rh, dosed with 50 Torr of ^{13}CO gave no NMR signal, indicating no adsorption (chemical or physical) of CO on the support, consistent with adsorption isotherm measurements at 300 K.

C. ^{13}C Relaxation Times of CO Adsorbed on Rh

A second 2.2% Rh on Al_2O_3 sample was prepared and progressively charged with ^{13}CO to a pressure of ~50 Torr at 300 K. The infrared spectra for precisely this sample were reported in Figure 5 of Reference 14. The NMR tube was separated from the infrared cell under ~50 Torr of ^{13}CO and stored at 300 K for 13 months.

The observed ^{13}C magnetization of this aged sample versus τ, the delay between the 180° prepulse and the 90° pulse, is plotted in Figure 3. If the ^{13}C nuclei had a single, spatially uniform T_1, the magnetization as a function of τ would form a straight line when plotted as in Figure 3. The data in Figure 3 can be fit within experimental error limits by assuming that the ^{13}C nuclei are separated into two types, with two distinct T_1's. The theoretical

equation describing the magnetization as a function of τ and the cycle time for this two-group model is:

$$M = M_o \left[\alpha_a e^{-\tau/T_{1a}} \left(1 - e^{-t_c/T_{1a}} \right) + \alpha_b e^{-\tau/T_{1b}} \left(1 - e^{-t_c/T_{1b}} \right) \right]$$

where M is the magnetization observed with a delay τ for measurements repeated after time t_c; α_a and α_b are the fractions of ^{13}C nuclei with spin-lattice relaxation times T_{1a} and T_{1b}, respectively; and M_o is the equilibrium ^{13}C magnetization. A least-squares fit of this equation to the data in Figure 3 indicates that, for this sample at 300 K, 42 ± 1% of the ^{13}C nuclei have a T_1 of 5.6 ± 0.4 msec, 58 ± 1% have a T_1 of 64 ± 4 msec, and $M_o = 4.44 \pm 0.04 \times 10^{19}$ ^{13}C nuclei, yielding a CO-to-Rh ratio of 1.04. When the experiment is repeated at 80 K, a least-squares fit of the data to the two-group model indicates that 43 ± 1% of the ^{13}C nuclei have a T_1 of 33 ± 3 msec and 57 ± 1% have a T_1 of 0.78 ± 0.08 sec. T_1 measurements on other 2.2% Rh on Al_2O_3 samples show that the relaxation times and site distributions are independent of the equilibrium pressure of ^{13}CO, in the range 50 to 10^{-3} Torr.

The lineshapes of the ^{13}C NMR spectra vary as τ increases, illustrated by representative spectra in Figure 4. One observes that the peak at ~-165 ppm disappears relatively quickly, while the shoulder at ~-280 ppm remains intact longer. With the relative proportions calculated from the T_1 data, the ten spectra associated with the data points in Figure 3 may be decomposed into the two basis spectra corresponding to the two different T_1's. A least-squares deconvolution yields the two spectra shown in Figure 5. Although this aged sample is composed of a greater percentage of short T_1 ^{13}C nuclei than fresh samples, the spectrum for the specie with T_1 = 5.6 msec, Figure 5(a), still

contains a relatively high noise level because the signal decays rapidly with τ, and thus the computed spectrum is determined by relatively fewer experimental spectra. The data of Figure 5(a) are fit with a Lorentzian function with 1.85 KHz full width at half maximum. The centers of mass of the two generated spectra are -177 ± 7 ppm and -199 ± 7 ppm for the species with T_1's of 5.6 msec and 64 msec, respectively. The signal-to-noise ratios for the spectra at 80 K prohibited a meaningful decomposition into the basis spectra at that temperature.

D. Exchange of $^{12}CO(g)$ with $^{13}CO(ads)$

Previous infrared studies have shown that adsorbed ^{13}CO exchanges readily and extensively with $^{12}CO(g)$ at 300 K (14). In addition, it is possible to exchange selectively only the $Rh(^{13}CO)_2$ specie by cooling the substrate to temperatures lower than 200 K and then exposing to ^{12}CO (15,32). Further studies on CO adsorbed on Rh on Al_2O_3 reveal that upon warming the selectively exchanged sample from 200 K to 300 K, complete isotopic mixing between CO adsorbed on all sites on the surface occurs on the order of hours, even at CO pressures below $\sim 10^{-3}$ Torr (33).

By studying these exchange phenomena with ^{13}C NMR, it is possible to determine quantitatively the site distribution of adsorbed CO. A freshly prepared sample of 2.2% Rh on Al_2O_3 was exposed to ~50 Torr of ^{13}CO at 300 K and allowed to equilibrate for two days. After reducing the CO pressure to 10^{-2} Torr, the infrared scan of the sample was similar to spectra previously reported, e.g., Figure 5 of Reference 14. The integrated intensity of the NMR spectrum indicates a CO-to-Rh ratio of 0.82 ± 0.02. The ^{13}C T_1's of this sample were measured as before and, assuming a two-group model, were found to be distributed as 34 ± 1% with T_1 equal to 4.0 ± 0.2 msec and 66 ± 1% with T_1 equal to 34 ± 2 msec. The ratio of short to long T_1's in the freshly prepared smple (34:66) was less than that of the 13-month-old sample (42:58). Concurrently,

the overall CO-to-Rh ratio as measured by the NMR varied from 0.82 for the fresh sample to 1.04 for the aged sample.

The freshly prepared NMR sample was cooled to 195 K in a dry ice/acetone bath and then exposed to ~50 Torr ^{12}CO, such that the ratio of $^{12}CO(g)$ to exchangable (at 195 K) $^{13}CO(ads)$ was ~45. (The present configuration of the equipment does not afford simultaneous low temperature experiments on the NMR and infrared samples.) After one hour, the CO pressure was reduced to 10^{-3} Torr over a 20 minute period; then the sample was allowed to warm while constantly pumping with a 20 liter/sec ion pump. After warming to 300 K, the sample was stored under an equilibrium CO pressure of 5×10^{-3} Torr.

After the low temperature exchange, the equilibrium magnetization of this sample had decreased by 33 ± 1%. Thus, 33% of the ^{13}CO adsorbed on the Rh on Al_2O_3 exchanged with the $^{12}CO(g)$ at 200 K and was evacuated from the sample. After the exchange the ^{13}C T_1's were distributed as 31 ± 1% with a T_1 of 2.4 ± 0.2 msec and 69 ± 1% with a T_1 of 43 ± 4 msec. Thus, decreasing the ^{13}C-isotopic enrichment of the adsorbed CO from 90% to 70% causes the rapidly relaxing group to relax more quickly and the relatively slower relaxing group to relax more slowly. In addition, the new distribution (31:69) is almost the same as the original distribution (34:66). This distribution was measured after the system had sufficient time to isotopically scramble from ~100% ^{12}CO on the dicarbonyl site and 10% ^{12}CO on the Rh rafts to a uniform $^{13}CO/^{12}CO$ ratio on both the dicarbonyl and raft sites, as observed by infrared spectroscopy. Because of the extended period of time required to measure the T_1 distribution, it was not possible to complete the NMR measurements at 300 K immediately after the exchange, nor was it feasible to maintain temperatures of 200 K for the duration of the experiment. Consequently, it was not possible to determine with NMR spectroscopy if the exchange selectively removed ^{13}CO

from one T_1 group (i.e., almost all the ^{13}CO of the short T_1 group or about half the longer T_1 group) which subsequently redistributed upon warming, or if the exchange was equally distributed among the two T_1 groups.

IV. DISCUSSION

A. ^{13}C Relaxation Mechanism for ^{13}CO Adsorbed on Rh

The ^{13}C T_1's of the ^{13}CO adsorbed on Rh dispersed on Al_2O_3 are between 2 and 64 msec in the two samples examined. These extremely short T_1's are typical of relaxation from paramagnetic centers. Other relaxation processes, such as fluctuating dipolar interactions from neighboring ^{27}Al or ^{1}H spins of the substrate typically yield ^{13}C T_1's of many seconds or more. The Al_2O_3 contains a relatively high level of Fe impurities, 0.2% by weight. The electron paramagentic resonance spectrum indicates that the Fe is distributed throughout the sample, rather than clustered in metallic particles, and is present as Fe^{++}. The rapidly fluctuating magnetic fields from the unpaired electrons of these Fe ions can relax nuclei in the sample by three mechanisms, depending on the mobility of the unpaired electrons and the nuclei of interest. First, if the unpaired electron is confined to the metal atom and the ^{13}C nuclei are spatially fixed, the ^{13}C nuclei very close to the metal atoms will relax rapidly and then equilibrate with the other ^{13}C nuclei via ^{13}C-^{13}C mutual spin flips. Second, if the molecules containing the ^{13}C diffuse rapidly through the sample, each ^{13}C nucleus may be individually relaxed by contacting the paramagnetic center. Third, the unpaired electrons may interact directly with each ^{13}C nucleus if the electrons are free to move through the lattice to the ^{13}C adsorption sites.

Although it is not possible at present to determine which mechanism or combination of mechanisms is causing the ^{13}C spin-lattice relaxation, one can

eliminate some possibilities due to the nature of the sample or the consequences of the models invoked. For example, it is inconceivable that the unpaired electrons are able to translate freely through an insulator such as Al_2O_3. Also, the desorption studies have shown that the CO does not diffuse through the sample by desorbing into the gas phase and then readsorbing onto a different site. (However, this does not rule out exchange between sites on a single raft.) Homonuclear ^{13}C-^{13}C spin flips are too slow to account for the rapid dissemination of relaxation through the sample because of long internuclear distances between different rafts or carbonyl sites.

A random distribution of Fe^{++} in the Al_2O_3 lattice yields an average ^{13}C-Fe^{++} separation of ~35 Å, which is sufficient to allow direct relaxation between fixed sites. Such a random distribution of lengths and orientations relative to the external magnetic field of the ^{13}C-Fe^{++} internuclear vector could result in an inhomogeneous T_1 for the ^{13}C nuclei. If both the ^{13}C nuclei and the Fe^{++} paramagnetic centers are fixed, the ^{13}C T_1 is given by the following equation (34):

$$\frac{1}{T_1} = 6 \frac{\gamma_c^2 \gamma_e^2 \hbar^2}{r^6} \sin^2\theta \cos^2\theta \left[\frac{T_{1e}}{1 + \omega_c^2 T_{1e}^2}\right]$$

for an internuclear vector of length r at an angle θ to the external magnetic field, γ_i is the respective gyromagnetic ratio, T_{1e} is the electron spin-lattice relaxation time, typically 10^{-6} to 10^{-7} s at 300 K, and ω_c is the carbon Larmor frequency. One can derive an expression for the number of spins as a function of T_1, i.e., $N(T_1)$, from the above equation. The magnetization as a function of τ, the delay between the 180° and 90° pulses, is given by the following equation:

$$M(\tau) = \int_0^{T_{1,max}} e^{-\tau/T_1} N(T_1) dT_1$$

This model for $N(T_1)$ yields an $M(\tau)$ that decreases approximately exponentially with τ, yielding a straight line with a slight concave downward shape when plotted as in Figure 3. Although not shown, this results in a very poor fit to the experimental data. In addition, the isotropic chemical shifts of the two T_1-resolved spectra differ by 22 ppm. In an amorphous sample, the unpaired electron of one atom may cause the broadening of the NMR lineshape of the nucleus of a different atom but not a shift in the overall frequency (35). Thus, the difference in chemical shifts between rapidly and slowly relaxing nuclei indicates that the two T_1 types are chemically distinct and not the results of a random site formation near the Fe^{++} paramagnetic centers. This does not rule out the possibility that the Rh preferentially congregates at the paramagnetic sites. Although it is possible to postulate a nonrandom distribution of paramagnetic impurities to fit the T_1 data, we believe it is very unlikely that the Rh would selectively distinguish between the FeO and Al_2O_3 sites of the substrate when the Rh is deposited as $RhCl_3$ or when later reduced since there are only 2 atoms of Fe per 1000 Al atoms.

The current data do not allow one to deduce the principal NMR relaxation process and, more specifically, why there is a distribution of ^{13}C T_1's. However, as introduced earlier in this paper, the T_1 data can be fit with a model that assumes there are two types of adsorbed ^{13}CO, each with distinct T_1's. The interpretation and justification of this two-group model will be discussed in the next section. This model assumes that $N(T_1)$ is the sum of two delta functions at T_{1a} and T_{1b}, with relative areas α_a and α_b, which yields an $M(\tau)$ that is the sum of two exponentials (for adequately slow pulse rates). For negligible cross-relaxation and molecular exchange between groups, which is the

case for this dilute ^{13}C system, α_a and α_b represent the relative populations of the two T_1 groups. The fit of this model is not improved within error limits by increasing the number of T_1 types to three or more. Also, this simple model assumes that ^{13}C nuclei have T_1's of precisely T_{1a} or T_{1b}, which is probably not the case with this amorphous, inhomogeneous sample. Rather, there is more likely two distributions of T_1's centered at T_{1a} and T_{1b} which would more accurately be modeled by two finite width Gaussian peaks rather than two delta functions.

B. Interpretation of the T_1-resolved ^{13}C NMR Spectra

As discussed in the introduction, previous infrared studies have established three states of CO adsorbed on dispersed Rh. Of these three states, the linear and bridged bonded CO (species II and III) would be expected to have the same ^{13}C T_1's because of rapid interconversion and diffusion of CO states on the raft and the same exposure to nearby paramagnetic centers in the substrate lattice. Thus, in terms of the infrared-identified states, the two ^{13}C T_1 types would be assigned to CO on a single Rh (specie I) and CO on the Rh rafts (species II and III). This interpretation of the two T_1 types as well as the assignment of the two T_1-resolved NMR spectra in Figure 5 is supported by the chemical shift information, the results of the quantitative selective $^{12}CO(g)/^{13}CO(ads)$ exchange, and the T_1 distribution as a function of the overall ratio of CO(ads) to Rh.

The isotropic chemical shifts of the two T_1-resolved spectra are -177 ppm for the 5.6 msec T_1 spectrum (Figure 5(a)) and -199 ppm for the 64 msec T_1 spectrum (Figure 5(b)). Recall that the difference of 22 ppm between the two T_1 types indicates that the two T_1 types are chemically distinct. The chemical shifts of various rhodium carbonyl compounds are given in Table I. The isotropic chemical shift of CO is -181.3 ppm. The model compound for the surface dicarbonyl specie, $Rh_2Cl_2(CO)_4$, has a chemical shift anisotropy comparable to the computed static

value for CO (36) and a very slight shift in the center of mass to -180 ppm. The isotropic chemical shifts of CO bonded as a terminal group on various rhodium complexes range from -176 to -192 ppm, with an average at about -184 ppm. The bridged bonded state of CO has the largest change in chemical shift, ranging from -212 to -236 ppm, with an average at about -228 ppm.

The ^{13}C NMR lineshape of CO adsorbed on the Rh rafts will contain contributions from the linear and bridged sites. The isotropic chemical shift of the longer T_1 specie, -199 ppm, lies in the range of shifts between the linear and bridged values. The isotropic chemical shift of the specie with the 5.6 msec T_1 is 22 ppm upfield at -177 ppm, which is closer to that of the dicarbonyl state. Thus, based on the isotropic chemical shifts, we assign the lineshape with the T_1 of 5.6 msec to ^{13}CO adsorbed in the dicarbonyl state (specie I) and the lineshape with the T_1 of 64 msec, Figure 5(b), to the ^{13}CO adsorbed on the Rh rafts (species II and III).

The isotropic chemical shift of the ^{13}C spectrum of CO on the rafts is a linear combination of the isotropic shifts of the linear and bridged states. Assuming that the chemical shifts of the linear and bridged species are similar to those of the model compounds, -184 and -228 ppm, respectively, the observed isotropic shift of Figure 5(b), -199 ppm, yields an estimated CO distribution of 66% linear states and 34% bridged states. Thus, based on the chemical shift data, the CO is distributed on this aged sample as 42% dicarbonyls (specie I), 38% linear bonded (specie II), and 20% bridged bonded (specie III).

The results of the $^{12}CO(g)/^{13}CO(ads)$ exchange at 200 K support the assignment of the two T_1 types to CO adsorbed as a dicarbonyl and CO adsorbed on the Rh rafts. Recall that infrared studies have demonstrated that the $Rh(^{13}CO)_2$ specie exclusively and extensively exchanges with $^{12}CO(g)$ at temperatures below 200 K (15). The NMR revealed that for a sample in which 34% of the ^{13}CO was

adsorbed in the short T_1 state and 66% was adsorbed in the longer T_1 state, the low temperature ^{12}CO exchange removed 33% of the adsorbed ^{13}CO. The NMR also found that the remaining ^{13}CO was proportionately distributed among the two T_1 types. Recall that infrared results predict that the surface sites would isotopically scramble within hours upon warming. Thus, it could not be demonstrated experimentally that the specie with the shorter T_1 was exclusively removed during the exchange. However, the agreement between the amount of ^{13}CO removed and the amount of ^{13}CO originally in the shorter T_1 group strongly suggests that the CO adsorbed as dicarbonyls has the shorter T_1's. A fresh sample was chosen for the exchange study because the ratio of species with different T_1's was more pronounced than in the aged samples and thus made it easier to assign the amount exchanged to a specific group.

Finally, consider the distribution between the T_1 groups as a function of the overall CO-to-Rh ratio. A freshly prepared sample with an overall CO-to-Rh ratio of 0.82 had 34% of the ^{13}C in a short T_1 state and 66% in the longer T_1 state. The aged sample had a higher ratio of CO-to-Rh at 1.04, and the T_1 distribution changed from 34:66 to 42:58. Since the aged sample actually has more CO on the surface and not just a redistribution of CO, it is not possible to calculate individual CO/Rh ratios for the two T_1 groups. However, assuming that the two T_1 groups are Rh dicarbonyls and CO on Rh rafts, it is possible to calculate the consequences of pairing these species to the two T_1 groups. Assigning the longer T_1 species to the dicarbonyl requires that at least 36% of the Rh on the fresh sample and at least 12% of the Rh on the aged sample be inactive. Assigning the shorter T_1 specie to the dicarbonyl requires that at least 14% of the Rh on the fresh sample be inactive, but all of the Rh on the aged sample may be active. The hydrogen uptake and the degree of dispersion of Rh measured in other studies (16,18), indicates that the latter assignment

is correct, consistent with previous arguments.

C. Molecular Motions of CO Adsorbed on Rh

The two ^{13}C NMR lineshapes of adsorbed CO in Figure 5 are radically different from the rigid chemical shift powder patterns of the model compounds, such as the $Rh_2Cl_2(CO)_4$ spectrum in Figure 1 or the $Rh_6(CO)_{16}$ spectrum of Reference 31. The spectra of the adsorbed CO broaden when the sample is cooled from 300 K to 80 K, as shown in Figures 2(a) and 2(b), indicating that at 300 K the spectrum is narrowed by molecular motions at frequencies greater than or equal to the NMR linewidth, i.e., a few KHz. The residual broadening at 80 K is probably the result of heteronuclear interactions with ^{27}Al and ^{1}H and the heterogeneity of the adsorbed states. Since the ^{13}C NMR spectrum does not broaden when the CO pressure is reduced from 50 to 10^{-6} Torr, the major averaging mechanism is not rapid exchange with the gas phase, i.e., $CO(g) \rightleftarrows CO(ads)$. Rather, the narrowing of the spectra in Figure 5 is due to motion localized at the individual adsorption sites.

The possible localized motions of adsorbed CO are different on the Rh dicarbonyl site compared to the Rh raft sites. The motions predicted to be in the frequency range of interest are reorientation about the axis bisecting the OC-Rh-CO angle of the dicarbonyl and surface diffusion of CO from site to site within the Rh raft boundaries. The characteristic effects on the chemical shift powder pattern of rotations and site exchange have been studied previously (40,41). Spiess (40) has shown that when molecules exchange between equivalent sites at correlation times on the order of the chemical shift anisotropy, the axisymmetric powder pattern retains the full anisotropy but decreases in intensity at the extreme frequencies of the tensor and increases in the frequency range between the prependicular tensor component and the isotropic frequency.

For an illustration of the effects of site exchange on a rigid NMR lineshape, see Figure 4 of Reference 40. Reorientation about a rotation axis has a distinctly different effect on the NMR lineshape. For intermediate correlation times, Sillescu (41) has shown that random reorientation about a rotation axis causes the observed anisotropy of the NMR lineshape to collapse as the correlation time decreases. As opposed to exchange between sites, this rotation causes no new structure to develop in the lineshape. This is the case illustrated in Figures 1 to 3 of Reference 41. For rapid molecular reorientation, both rotation and site exchange cause the line to collapse to a Lorentzian curve; thus, in this limit it is not possible to identify the type of motion present in the sample.

The ^{13}C NMR spectrum assigned to the dicarbonyl surface specie, Figure 5(a) has been fit with a Lorentizan curve with a linewidth of 1.85 KHz. Fitting a Gaussian curve to these data results in a mean square deviation three times that of the Lorentzian fit. The noise level in the spectrum does not permit an accurate determination of the ratio of the fourth moment to the second moment squared, which is usually used to differentiate between the two characteristic lineshapes (42). The Lorentzian shape of the spectrum in Figure 5(a) indicates that the narrowing of the spectrum is principally the result of motional averaging, as opposed to homogeneous broadening responsible for Gaussian curves (42). The ratio of the Lorentzian linewidth to the anisotropy of the ^{13}C NMR spectrum of the model compound $Rh_2Cl_2(CO)_4$ is about 0.3. For this narrowing there still exist subtle differences in the lineshapes caused by the effects of the rotation and site exchange models; however, the high noise level prohibits any such differentiation. The most probable motion for the dicarbonyl specie is reorientation of the two CO molecules about an axis perpendicular to the Al_2O_3 surface. The correlation time of the rotation

computed from the linewidth is approximately 0.5 msec at 300 K.

Thus, the ^{13}C NMR spectrum indicates that the single Rh atom is present on the Al_2O_3 surface such that the CO groups and the Rh atom itself are relatively free to rotate to new orientations. In the rhodium carbonyl compounds where the Rh atom forms multiple bonds with the complex, e.g., two Rh-Cl bonds in $Rh_2Cl_2(CO)_4$ and four Rh-Rh bonds in $Rh_6(CO)_{16}$, the ^{13}C NMR powder pattern shows no evidence of motions on the order of a few KHz. As the carbonyls of the $Rh(CO)_2$ site are relatively unrestricted to reorient, it implies that the bonding of the Rh atom to the Al_2O_3 is more axially symmetric than in the model compounds. Possible models for this situation would be a Rh atom bonded to the support through a single bond, such as to an oxygen atom, or an Rh atom physisorbed on the Al_2O_3 such that the weak bonding does not orient the Rh-CO bonds.

The ^{13}C NMR lineshape assigned to the CO adsorbed on the Rh rafts, Figure 5(b), is the superposition of a powder pattern for the linear specie (three components near 80, -305 and -315 ppm) and a powder pattern for the bridged specie (two components at about -102 and -296 ppm) which would result in five structural features, assuming that none are coincident. Figure 5(b) has definite features at about -190, -250, and -300 ppm. The structure at -250 and -300 ppm may be assigned to the perpendicular components of the two overlapping chemical shift tensors, but the peak at -190 ppm is too far upfield to be a principal component of either of the tensors. Rather, the peak at about -190 ppm, close to the isotropic frequency of the linearly adsorbed CO, is characteristic of the effects of CO exchanging between sites on the Rh raft. Also, there is observable intensity over the entire range of the predicted anisotropy, 100 to -300 ppm, as expected by the site-exchange motional model. The features

at 80, 4, and -385 ppm are probably not real since they are comparable to the noise level and are accompanied by negative peaks in the other complimentary computed lineshape of Figure 5(a). Spectrum 5(b) does not allow a calculation of the rate of diffusion and activation energy for surface diffusion of CO on the Rh raft. The diffusion rate may be accurately computed only after a separation of the individual ^{13}C NMR spectra of the linear and bridged states and after the sources of the other broadening are quantified.

D. Distribution of Rh Atoms on Al_2O_3

The T_1 results for the aged 2.2% Rh on Al_2O_3 sample indicate that the CO is distributed on the surface as 42% bonded as dicarbonyls (specie I) and 58% adsorbed on the Rh rafts. The isotropic chemical shift of the ^{13}C NMR spectrum of the CO on the Rh rafts indicates that for this sample the ratio of linear to bridged states is 66 to 34. The overall CO-to-Rh ratio of 1.04 requires that for every 104 adsorbed CO molecules, there are 100 Rh atoms. The 44 CO molecules adsorbed as dicarbonyls are bonded to 22 Rh atoms, or 22% of the Rh on the Al_2O_3. The configuration of the Rh rafts may be determined by assuming a stoichiometry for the Rh-CO bonding on the rafts. If one assumes that a Rh atom linearly bonded to a CO makes no other bonds to CO molecules, the 60 CO molecules on the raft (40 linear and 20 bridged) will require 80 Rh atoms (40 + 40). The local ratio of CO to Rh atoms on the raft for this model is 60/80 = 0.75. It has been shown recently by low energy electron diffraction (43) that at full CO coverage on Rh(111) at temperatures of about 180 K, the ratio of CO to surface Rh atoms is 0.75. This model for the CO on the raft yields an overall CO-to-Rh ratio of 1.03, which is very close to the observed ratio of 1.04. However, the CO-to-Rh ratio of Reference 43 was measured at pressures less than 10^{-6} Torr. It is possible that the CO coverage on the Rh(111) would increase at pressures on the order of 50 Torr.

It is possible that some of the raft Rh atoms make multiple bonds to the adsorbed CO. The extreme case is to assume that the raft has only 40 Rh atoms involved in the bonding to the adsorbed CO, and the bridged CO simply fills the voids between the linear Rh-(CO) sites as is observed in most rhodium carbonyl complexes (28,37-39). In this case, to satisfy the CO-to-Rh ratio of 1.04, 38 of the 100 Rh atoms (38%) must be unavailable for CO adsorption. The H_2 uptake on a freshly reduced 2.2 % Rh on Al_2O_3 sample is only about 0.9, compared to values as high as 1.16 reported for Rh on Al_2O_3 samples (18), indicating that some of the Rh is inactive. The uninvolved Rh atoms may be the result of incomplete reduction of the $RhCl_3$, Rh atoms buried under the surface Rh atoms in the rafts, or Rh atoms trapped in pores rendered inaccessible during the reduction/outgassing procedure. D. J. C. Yates, et al. (18) do not report any infrared absorption in the 1870 cm^{-1} range for the adsorption of CO on a 1% Rh on Al_2O_3 sample where the Rh rafts are entirely two-dimensional, or "ultradispersed," as determined by hydrogen uptake and electron microscopy. This suggests that the presence of a bridged bonded state of CO indicates that the Rh raft is three-dimensional, thus covering a percentage of the Rh atoms. Thus, the actual structure of the Rh rafts on the 2.2% Rh on Al_2O_3 samples studied here is probably partially two-dimensional with some three-dimensional portions.

E. Estimation of Infared Absorption Coefficients for ^{13}CO on Rh

The absolute populations of the three adsorbed states of CO on 2.2% Rh on Al_2O_3 as determined by ^{13}C NMR may be used to calibrate the infrared absorption intensities. Using the analysis based on the chemical shift data described earlier, the CO adsorbed on the freshly prepared 2.2% Rh on Al_2O_3 sample with an overall CO-to-Rh ratio of 0.82 was distributed as 34% dicarbonyls,

44% linear states, and 22% bridged states. Unfortunately, it was not possible to obtain an infrared spectrum of the 13-month-old sample after aging. Although the peaks of the infrared spectrum overlap slightly, as shown in Figure 5 of Reference 14, the individual intensities may be obtained by assuming that the large peaks at 2056 and 1987 cm^{-1} (the symmetric and antisymmetric stretches of $Rh(^{13}CO)_2$) are symmetric about their respective maxima so that the valley between these peaks may be artificially created and subtracted from the peak at 2024 cm^{-1} (the linear specie). The background due to the ^{12}CO impurity was estimated from other studies. The molar integrated intensity of each peak, A, is given by the following equation (1):

$$A = \frac{2.303}{c\ell} \int \log_{10}\left(\frac{I_o}{I}\right) d\nu$$

where c is the molar concentration of the substrate computed from the ^{13}C NMR data, ℓ is the path length through the sample, and the integration is over the full width of the infrared peak. For this particular sample at 300 K under an equilibrium 90% ^{13}CO pressure of 50 Torr, the molar integrated infrared intensities are 74, 128, 26, and 85 (cm) ($mole^{-1}$) (10^6) ± 10% for the symmetric and antisymmetric stretches of the dicarbonyl, the linear state, and the bridged state, respectively. The molar intensity for CO(g) is only 5.4×10^6 (44). This dramatic increase in the infrared absorption by CO upon bonding to the surface has been reported previously by Seanor and Amberg (44). By measuring the amount of CO adsorbed with a quartz spring microbalance, they calculated molar integrated intensities of 60 and 27 (cm) ($mole^{-1}$) (10^6) for CO chemisorbed on Pt on SiO_2 at 2100 and 2095 cm^{-1}, respectively. These infrared intensities chemisorbed CO are also very comparable to those of many metal carbonyls (45).

The molar integrated intensities reported here are for only one loading of Rh on Al_2O_3 at one coverage of CO. Recent infrared studies indicate that these values change as a function of loading in the range 0.2% to 10% Rh by weight on Al_2O_3 (46). UPS studies have shown that as the loading of Pd on a carbon substrate increases, the Pd cluster properties change from atomic to metallic behavior, which results in changes in the CO bonding to the Pd rafts (47). It is conceivable that the Rh rafts on Al_2O_3 may vary similarly with increased metal loading. In addition, preliminary ^{13}C NMR results suggest that at constant Rh loading, the molar integrated intensities of the adsorbed CO are inhomogeneous, varying as much as a factor of five for the dicarbonyl sites (48).

Further combined infrared and NMR studies as a function of ^{13}CO coverage and Rh loading are needed. It will also be possible to calculate the molar intensities for ^{12}CO adsorbed on Rh by measuring the site distributions of ^{13}CO by NMR and then measuring the infrared spectrum of ^{12}CO adsorbed on an identical sample. Calibration over the complete adsorption isotherm would be extremely useful in future sample characterization since the infrared spectra are relatively easier and faster to obtain than are NMR spectra.

F. Evidence for Isolated Rh Atoms on Al_2O_3

The doublet in the infrared spectrum of CO adsorbed on Rh at 2101 cm^{-1} and 2032 cm^{-1} has been assigned to two ^{12}CO molecules adsorbed to a single Rh atom, based on analogies to the infrared spectra of $Rh_2Cl_2(CO)_4^-$ and $Rh_2Br_2(CO)_4$ (13,27,49). This dicarbonyl specie is believed to form on either Rh atoms at the edge of the Rh rafts on the Al_2O_3 (18) or at single Rh atoms isolated from the Rh rafts (13,14,17). The cumulative evidence to date in support of the isolated Rh atoms is the following:

(1) The absorption at 2101 cm^{-1} and 2032 cm^{-1} do not shift to higher wavenumbers as the coverage of CO increases, as do the bands due to the linear

and bridged CO species adsorbed on Rh rafts (13,14). Thus, intermolecular CO-CO interactions at the dicarbonyl sites, through metal and through space, do not increase with CO coverage, indicating that these sites are isolated.

(2) The catalytic decomposition of H_2CO on Rh dispersed on Al_2O_3 forms primarily $Rh(CO)H_2$ and not $Rh(CO)_2$ (20). However, the $Rh(CO)_2H$ specie forms from $Rh(CO)H_2$ readily upon subsequent exposure to CO(g). If the dicarbonyl site were on the edge of a raft, surface diffusion would allow the dicarbonyl to form from the migration of CO(ads) from the decomposition of H_2CO on other Rh sites of the raft. Since it does not, it suggests that the Rh atoms are isolated from the rafts.

(3) The exchange of $^{12}CO(g)$ with ^{13}CO adsorbed on the Rh dicarbonyl sites at 200 K without the exchange of the ^{13}CO on the rafts suggests spatial isolation of the Rh atoms (15).

(4) The ^{13}C spin-lattice relaxation times of the adsorbed ^{13}CO are an order of magnitude different for the ^{13}CO on the Rh dicarbonyl sites compared to the ^{13}CO on the rafts. Such a difference in T_1's is possible only for ^{13}CO on Rh atoms isolated from the ^{13}CO on the Rh rafts.

Thus, the results from infrared spectroscopy, H_2CO adsorption, selective exchange and ^{13}C NMR support the conclusion that isolated Rh atoms exist on the Al_2O_3 surface. Knözinger, et al. have made an isotopic infrared study of the adsorption of $Rh_6(CO)_{16}$ onto ligand-modified silica substrates (50). The $Rh_6(CO)_{16}$ decomposes upon adsorption to form $Rh(CO)_2$ groups as evidenced by only a doublet in the initial infrared spectrum. Based on the results of partial isotopic exchange of $^{13}CO(g)$ and $^{12}CO(ads)$ and the absence of linear and bridged species at high CO coverages, Knözinger et al. concluded that the dicarbonyl groups are isolated from each other.

V. CONCLUSIONS

^{13}C NMR has been combined with infrared spectroscopy to characterize the adsorbed states of CO on Rh dispersed on Al_2O_3. The ^{13}CO is adsorbed on the dispersed Rh in two groups, characterized by ^{13}C T_1's an order of magnitude different. With respect to the states of adsorbed ^{13}CO identified by previous infrared studies (13-18), the two T_1 groups are interpreted to be ^{13}CO adsorbed on isolated Rh atoms as a dicarbonyl and ^{13}CO adsorbed on Rh rafts. Combining the T_1 data with the isotropic chemical shifts of the lineshapes, the ^{13}CO site distributions (dicarbonyl: linear: bridged) were found to be 42:38:20 for an aged 2.2% Rh on Al_2O_3 sample and 34:44:22 on a freshly prepared 2.2% Rh on Al_2O_3 sample. These site distributions may then be used to calculate the molar integrated intensities of the infrared spectra. The ^{13}C NMR may now be used directly to observe changes in the CO distribution caused by various surface treatments or indirectly by calibrating the infrared spectra of model samples.

The mobility of the adsorbed CO may also be obtained through NMR studies. This study has suggested two distinct motions of CO adsorbed on the surface. The CO adsorbed as a dicarbonyl is reorienting at the rate of a few KHz at 300 K, probably rotating about an axis bisecting the OC-Rh-CO angle. The CO on the Rh raft is exchanging between sites within the raft also at a rate on the order of a few KHz. Further quantification of these rates can provide information on the bonding of the Rh to the support and the degree of surface diffusion involved in the various reaction mechanisms of adsorbed CO. For example, Campbell and White have proposed that at temperature near 330 K, CO may react with O_2 over polycrystalline Rh via either Langmuir-Hinshelwood or Eley-Rideal mechanisms, where the later involves a mobile two-dimensional gaseous CO state (51).

The interpretation of the ^{13}C NMR results is being examined further by NMR studies such as magic-angle sample-spinning techniques (52) to resolve the isotropic chemical shifts of the three species and isolation of the spectra as a function of temperature to determine accurately the activation energies for local motions. In addition, the substrate may be modified to produce predictable changes in the relative amounts of isolated and raft Rh atoms, such as increasing the Rh loading on the Al_2O_3.

The introductory ^{13}C NMR investigation of the CO adsorbed on the Rh on Al_2O_3 system has provided the necessary background to understand the more complicated changes observed at elevated temperatures and in the presence of other molecules such as O_2 or H_2. We are currently undertaking the combined infrared and NMR studies of such systems.

VI. ACKNOWLEDGMENTS

While this study was in progress, Professor Robert W. Vaughan perished in a commercial airline crash in May of 1979. Bob's many contributions to the field of high-resolution solid state NMR include the development of improved multiple pulse schemes, dipole modulation techniques, double resonance interferometry, and NMR instrumentation. Bob applied these techniques to the study of a diverse group of materials including metal hydrides, metal carbonyls, hydrogen-bonded solids, superionic conductors, catalytic oxide surfaces, and molecules adsorbed on surfaces.

Bob Vaughan's generosity of spirit and intellect was beyond comparison. He gave unselfishly of his time and of himself to all worthwhile endeavors. In his personal life and his professional life, he constantly set high standards for himself and his co-workers, while always maintaining a refreshing modesty.

His enthusiasm was as boundless as it was contagious, and it was always fun to savor a new idea with Bob. We can only guess what the end result of his full career might have been, but we know that scores of intelligent young men and women will not have the benefit of his wisdom, his kindness, and his counsel. We have walked only a short distance with him, but our lives have each received that enrichment which can only come through knowing a truly good and kind friend.

The authors gratefully acknowledge support from the Office of Naval Research under contracts N00014-77-F-0008 and N00014-75-C-0960. We thank Professor G. R. Rossman for his generosity in allowing us to use his infrared spectrometer and G. W. Brudvig for measuring the electron paramagnetic resonance spectrum. Helpful comments and discussions were offered by S. I. Chan, W. H. Weinberg, and R. R. Cavanagh.

References

1. L. H. Little, Infrared Spectra of Adsorbed Species (Academic Press, London, 1966).
2. M. L. Hair, Infrared Spectroscopy in Surface Chemistry (Marcel Dekker, New York, 1967).
3. W. H. Weinberg, Ann. Rev. Phys. Chem. 29, 115 (1978).
4. R. W. Vaughan, Ann. Rev. Phys. Chem. 29, 397 (1978).
5. M. Mehring, High Resolution NMR Spectroscopy in Solids, Vol. 11 of NMR: Basic Principles and Progress (Springer-Verlag, New York, 1976).
6. U. Haeberlen, High Resolution NMR in Solids: Selective Averaging, Adv. Mag. Resonance Suppl. 1 (Academic Press, New York, 1976).
7. E. G. Derouane, J. Fraissard, J. J. Fripiat, and W. E. E. Stone, Catalysis Reviews 7, 121 (1972).
8. H. Pfeifer, NMR: Basic Principles and Progress 7 (Springer-Verlag, New York, 1972), p. 53.
9. T. M. Duncan, J. T. Yates, Jr., and R. W. Vaughan, J. Chem. Phys. 71, 3129 (1979).
10. J. B. Stothers, Carbon-13 NMR Spectroscopy (Academic Press, New York, 1972).
11. G. C. Levy, ed. Topics in Carbon-13 NMR Spectroscopy, Vol. 1 (Wiley, New York, 1974).
12. K. F. Lau and R. W. Vaughan, Chem. Phys. Lett. 33, 550 (1975).
13. A. C. Yang and C. W. Garland, J. Phys. Chem. 61, 1504 (1957).
14. J. T. Yates, Jr., T. M. Duncan, S. D. Worley, and R. W. Vaughan, J. Chem. Phys. 70, 1219 (1979).
15. J. T. Yates, Jr., T. M. Duncan, and R. W. Vaughan, J. Chem. Phys. 71, 3908 (1979).

16. M. Primet, J. Chem. Soc. Far. Trans. I, 74, 2570 (1978).

17. H. C. Yao and W. G. Rothschild, J. Chem. Phys. 68, 4774 (1978).

18. D. J. C. Yates, L. L. Murrell, and E. B. Prestridge, J. Catal. 57, 41 (1979).

19. R. M. Kroeker, W. C. Kaska, and P. K Hansma, J. Catal. 57, 72 (1979).

20. J. T. Yates, Jr., S. D. Worley, T. M. Duncan, and R. W. Vaughan, J. Chem. Phys. 70, 1225 (1979).

21. H. Arai and H. Tominaga, J. Catal. 43, 131 (1976).

22. R. W. Vaughan, D. D. Elleman, L. M. Stacy, W. K. Rhim, and J. W. Lee, Rev. Sci. Instrum. 43, 1356 (1972).

23. (a) H. Y. Carr and E. M. Purcell, Phys. Rev. 94, 630 (1954).

    (b) R. L. Vold, J. S. Waugh, M. P. Klein, and D. E. Phelps, J. Chem. Phys. 48, 3831 (1968).

24. H. S. Gutowsky, R. L. Vold, and E. J. Weld, J. Chem. Phys. 43, 4107 (1965).

25. S. A. Al'tshuler and B. M. Kozyrev, Electron Paramagnetic Resonance in Compounds of Transition Elements, 2nd ed., Eng. Trans. from Russian (John Wiley and Sons, New York, 1974), pp. 336-34[illegible].

26. J. B. Peri, J. Phys. Chem. 70, 1482 (1966).

27. C. W. Garland and J. R. Wilt, J. Chem. Phys. 36, 1094 (1962).

28. P. Chini, S. Martinengo, D. J. A. McCaffrey, and B. T. Heaton, J. C. S. Chem. Comm. 310 (1974).

29. N. Bloembergen and J. A. Rowland, Acta Metall. 1, 731 (1953).

30. H. W. Spiess, R. Grosescu, U. Haeberlen, Chem. Phys. 6, 226 (1974).

31. J. W. Gleeson and R. W. Vaughan, to be published.

32. The authors had previously reported low temperature $^{12}CO/^{13}CO$ exchange data with ambiguous results in the 1900 cm^{-1} region, suggesting a possible exchange of the bridged specie. Further infrared studies have confirmed that the effect was due to a shift in the background spectrum and not exchange.

33. T. M. Duncan, J. T. Yates, Jr., R. W. Vaughan (unpublished).

34. A. Abragam, The Principles of Nuclear Magnetism (Oxford University Press, London, 1961) Chapter IX.

35. Reference 34, Chapter VI.

36. A. A. V. Gibson and T. A. Scott, J. Mag. Resonance 27, 29 (1977).

37. B. T. Heaton, A. D. C. Towl, P. Chini, A. Fumagalli, D. J. A. McCaffrey, and S. Martinengo, J. C. S. Chem. Comm. 523 (1975).

38. J. Evans, B. F. G. Johnson, J. Lewis, J. R. Norton, and F. A. Cotton, J. C. S. Chem. Comm. 807 (1973).

39. J. Evans, B. F. G. Johnson, J. Lewis, and J. R. Norton, J. C. S. Chem. Comm. 79 (1973).

40. H. W. Spiess, Chem. Phys. 6, 217 (1974).

41. H. Sillescu, J. Chem. Phys. 54, 2110 (1971).

42. Reference 34, Chapter IV.

43. P. A. Thiel, E. D. Williams, J. T. Yates, Jr. and W. H. Weinberg, Surf. Sci. 84, 54 (1979).

44. D. A. Seanor and C. H. Amberg, J. Chem. Phys. 42, 2967 (1965).

45. T. L. Brown and D. J. Darensbourg, Inorg. Chem. 6, 971 (1967).

46. R. R. Cavanagh and J. T. Yates, Jr., to be published.

47. M. Grunze, Chem. Phys. Lett. 58, 409 (1978).

48. T. M. Duncan, PhD Thesis, California Institute of Technology, 1980.

49. L. F. Dahl, C. Martell, D. L. Wampler, J. Am. Chem. Soc. 83, 1761 (1961).

50. H. Knözinger, E. W. Thornton, and M. Wolf, J. Chem. Soc. Far. Trans. I 75, 1888 (1979).

51. C. T. Campbell and J. M. White, J. Catal. 54, 289 (1978).

52. J. Schaefer and E. D. Stejskal, J. Am. Chem. Soc. 98, 1031 (1976).

TABLE I. ^{13}C NMR Shieldings in Rhodium Carbonyl Complexes

Compound	Carbonyl Group[a]	Principal Shielding Tensor Components[b] σ_{11}	σ_{22}	σ_{33}	$\bar{\sigma}$	Reference
CO	gas	-	-	-	-181.3	(10)
	solid at 4.2 K	62.	-303.	-303.	-181.3[c]	(36)
$Rh_2Cl_2(CO)_4$	Terminal (2)	99.	-299.	-306.	-169.(-186.)[d]	This Work
		-	-	-	-180.4	(28)
$Rh_6(CO)_{16}$	Bridged (3)	-102.	-296.	-296.	-231.3	(31)
		-	-	-	-231.5	(37)
	Terminal (2)	80.	-305.	-315.	-180.0	(31)
		-	-	-	-180.1	(37)
$[Rh_{12}(CO)_{30}]^{2-}$	Bridged (2)	-	-	-	-211.5	(28)
	Bridged (3)	-	-	-	-237.4	(28)
	Terminal (2)	-	-	-	-186.3	(28)
	Terminal (2)	-	-	-	-186.1	(28)
	Terminal (2)	-	-	-	-183.4	(28)
$Rh_4(CO)_{12}$	Bridged (2)	-	-	-	-228.8	(38)
	Terminal (3)	-	-	-	-183.4	(38)
	Terminal (2)	-	-	-	-181.8	(38)
	Terminal (2)	-	-	-	-175.5	(38)
$Rh_2(h^5\text{-}C_5H_5)_2(CO)_3$	Bridged (2)	-	-	-	-231.8	(39)
	Terminal (1)	-	-	-	-191.8	(39)

(a) Numbers in parentheses are the number of CO molecules at a single Rh atom for the terminals, or the number of Rh atoms involved in the bridged states.

(b) ppm, relative to tetramethylsilane, (TMS)

(c) Ref. 36 reported only the chemical shift anisotropy, $\sigma_{11} - \sigma_{33} = 365$. The principal component values were computed by assuming an isotropic shift of -181.3 ppm. The anisotropy is believed to be averaged by rapid librational modes at 4.2 K. The computed static anisotropy is 406 ± 30 ppm.

(d) Value in parentheses is the computed center of mass, rather than the isotropic value from the lineshape fit.

FIGURE CAPTIONS

Figure 1. ^{13}C NMR spectrum at 300 K of $Rh_2Cl_2(CO)_4$ enriched to 20% ^{13}C. 6.89 ppm per data point. See Table I for the fitted chemical shift tensor components.

Figure 2. ^{13}C NMR spectra of (a) a 2.2% Rh on Al_2O_3 sample with ~50 Torr of ^{13}CO at 300 K; (b) same sample, cooled to 80 K after reducing the CO pressure to 0.02 Torr; and (c) model carbonyl compound $Rh_2Cl_2(CO)_4$, from Figure 1, added for comparison. All spectra taken with τ = 0.5 msec, 6.89 ppm per point.

Figure 3. Observed magnetization versus τ, the delay between the 180^o and 90^o pulses, of ^{13}CO on 2.2% Rh on Al_2O_3. The CO(ads)-to-Rh ratio for this sample was 1.04. Pulse sequences repeated were every 0.4 sec.

Figure 4. ^{13}C NMR spectra of ^{13}CO adsorbed on 2.2% Rh on Al_2O_3 (CO/Rh = 1.04), with τ at (a) 0.5 msec, (b) 8.0 msec, (c) 30.0 msec, and (d) 50 msec.

Figure 5. ^{13}C NMR spectra of ^{13}CO adsorbed on 2.2% Rh on Al_2O_3 generated by decomposing the spectra taken as a function of τ, based on relative proportions computed from the T_1 distribution. The spin-lattice relaxation times of the two basis spectra are (a) 5.6 msec and (b) 64 msec.

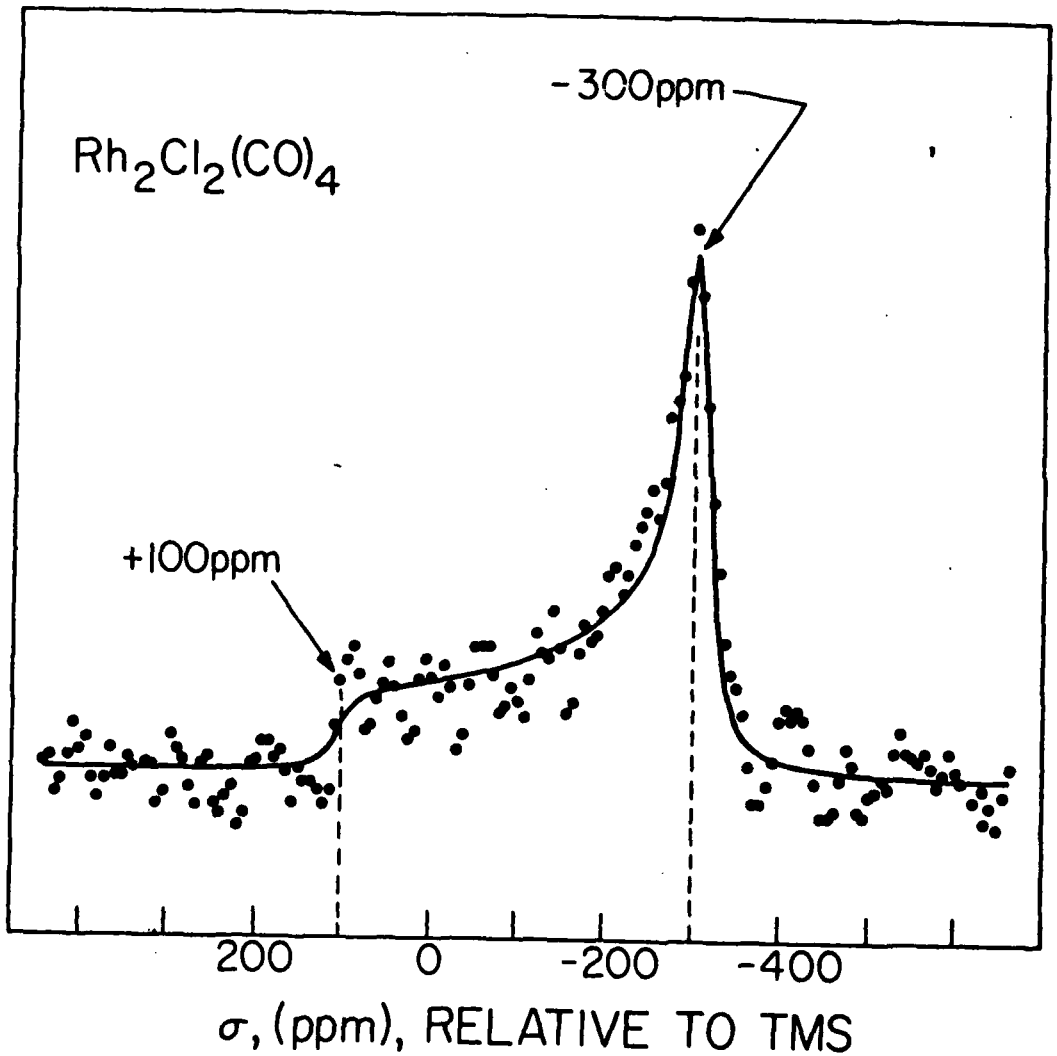

Figure 1

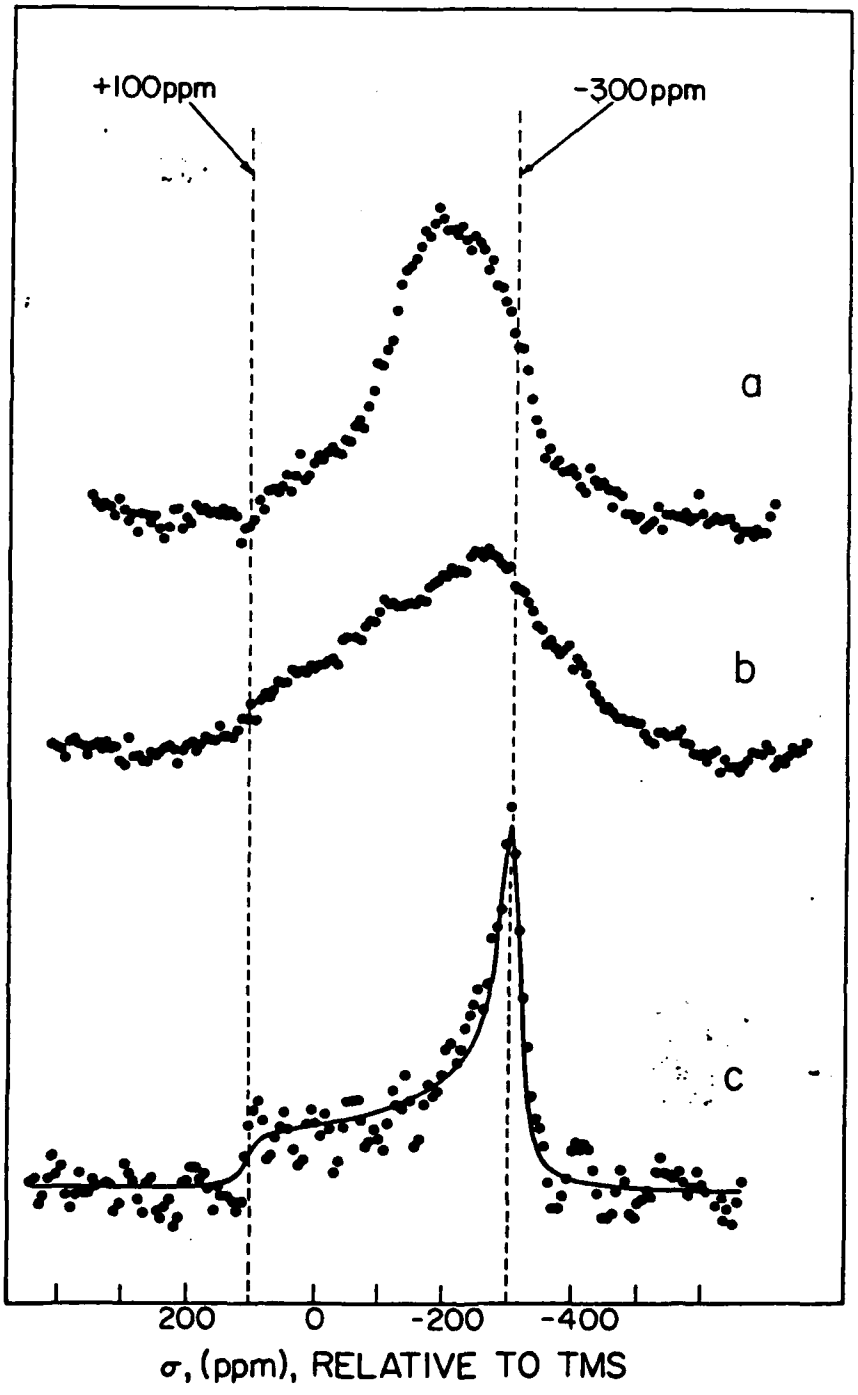

Figure 2

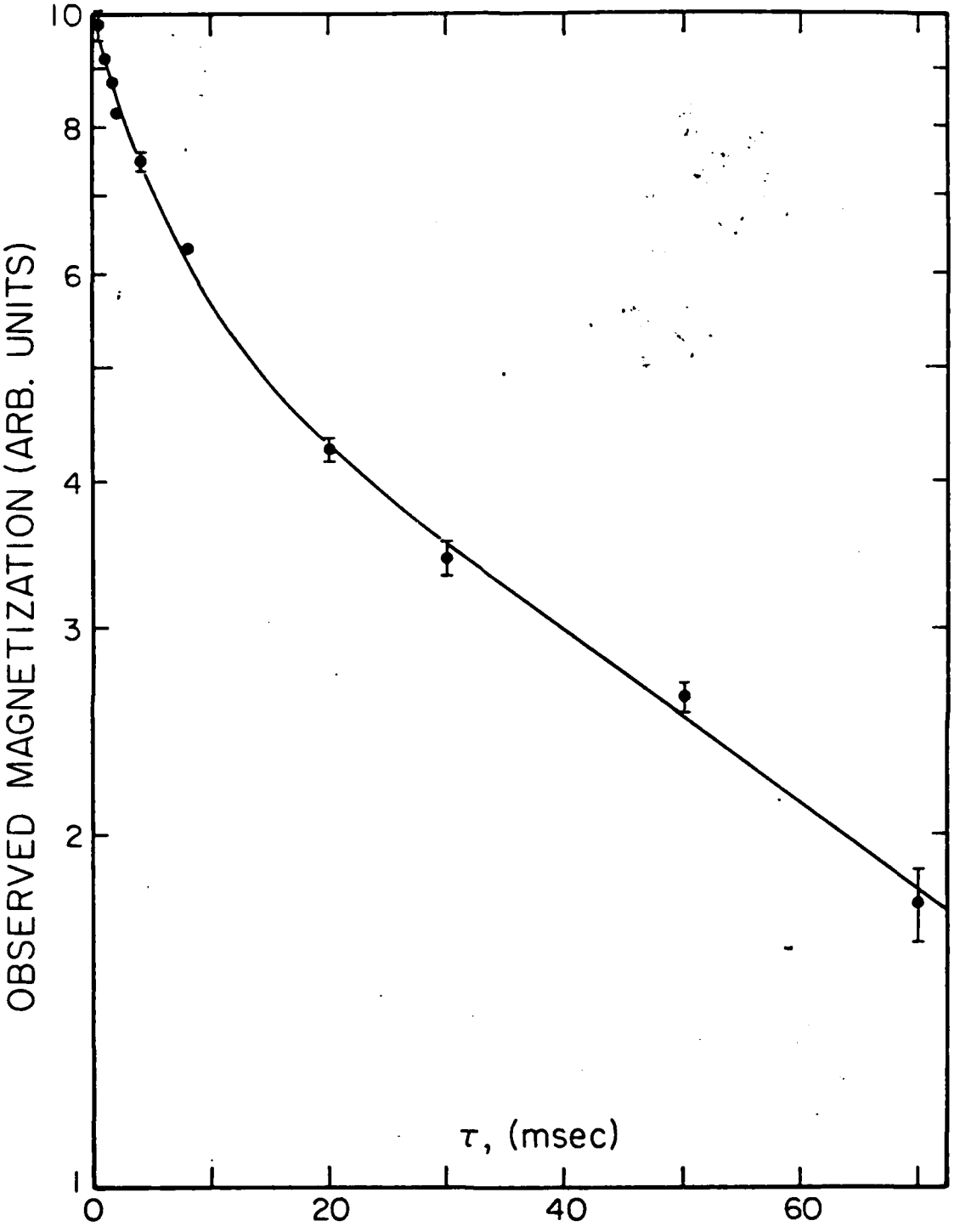

Figure 3

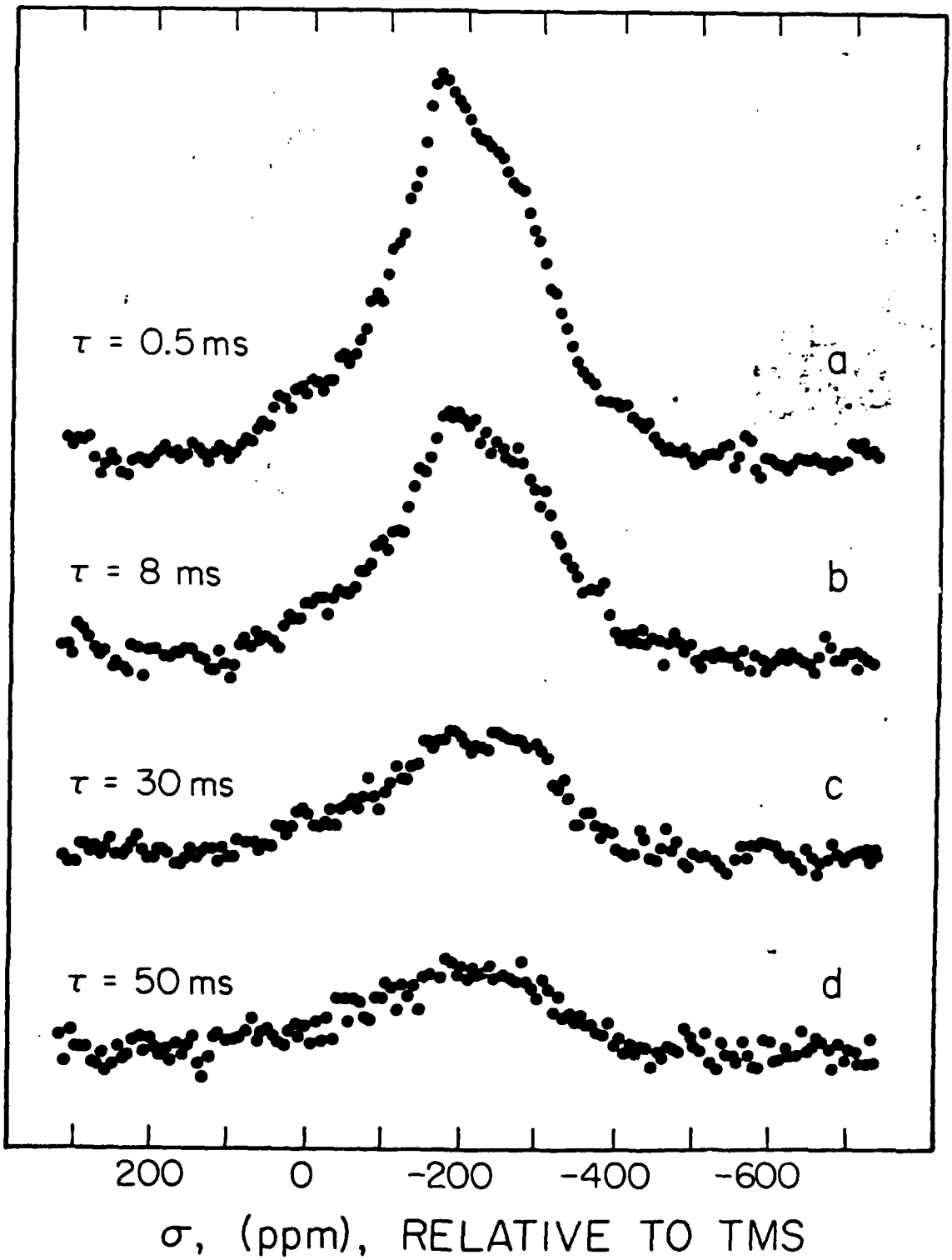
τ = 0.5 ms
a
τ = 8 ms
b
τ = 30 ms
c
τ = 50 ms
d
200
0
-200
-400
-600
σ, (ppm), RELATIVE TO TMS

Figure 4

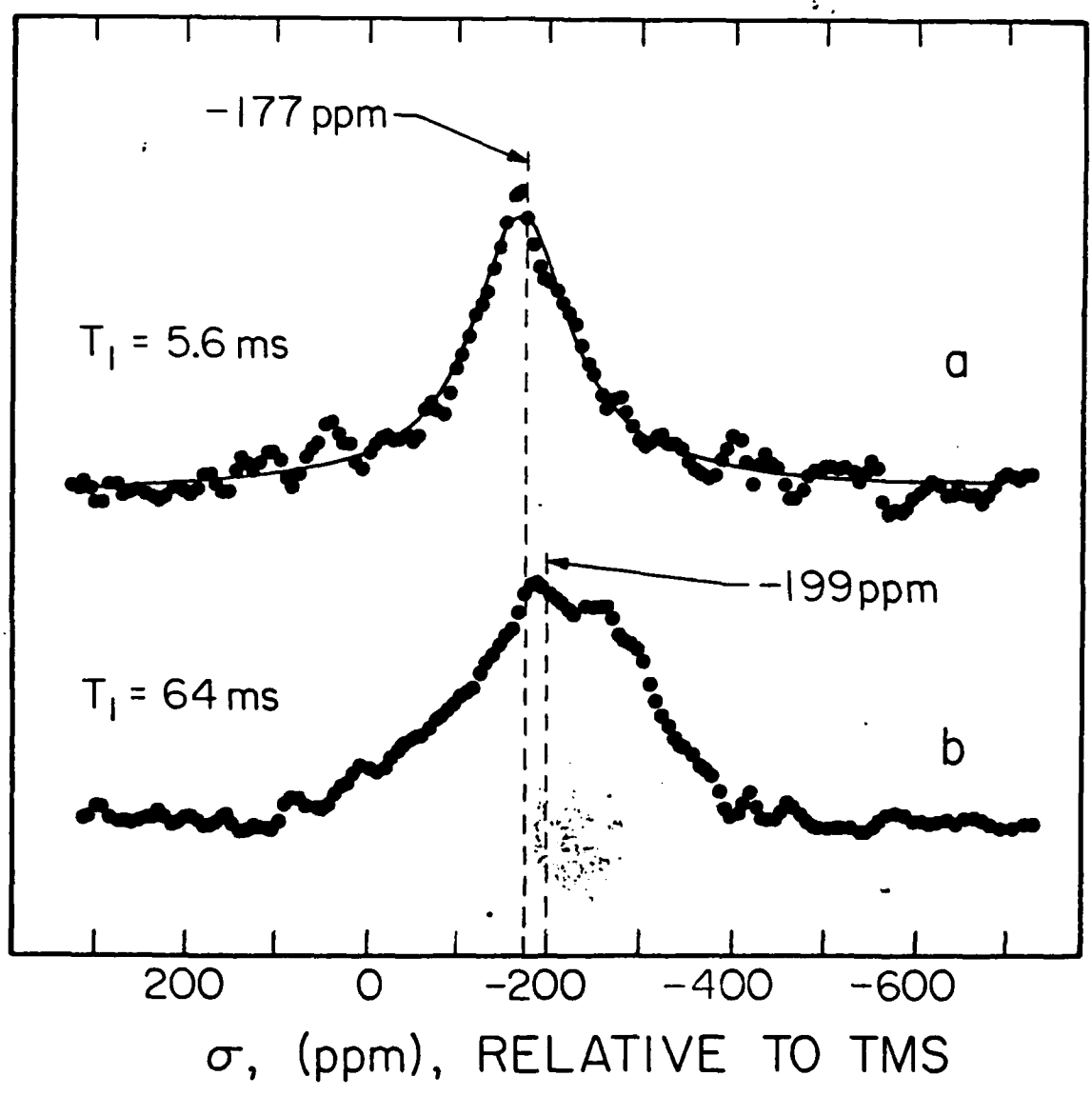
-177 ppm
T_1 = 5.6 ms
a
-199 ppm
T_1 = 64 ms
b
200
0
-200
-400
-600
σ, (ppm), RELATIVE TO TMS

Figure 5

UNCLASSIFIED

SECURITY CLASSIFICATION OF THIS PAGE (When Data Entered)

REPORT DOCUMENTATION PAGE		READ INSTRUCTIONS BEFORE COMPLETING FORM
1. REPORT NUMBER Technical Report #15	2. GOVT ACCESSION NO.	3. RECIPIENT'S CATALOG NUMBER
4. TITLE (and Subtitle) A ^{13}C NMR Study of the Adsorbed States of CO on Rh Dispersed on Al_2O_3		5. TYPE OF REPORT & PERIOD COVERED 6. PERFORMING ORG. REPORT NUMBER
7. AUTHOR(s) T. M. Duncan, J. T. Yates, Jr., and R. W. Vaughan		8. CONTRACT OR GRANT NUMBER(s) N00014-77-F0008 N00014-75-C960
9. PERFORMING ORGANIZATION NAME AND ADDRESS Division of Chemistry & Chemical Engineering California Institute of Technology Pasadena, CA 91125		10. PROGRAM ELEMENT, PROJECT, TASK AREA & WORK UNIT NUMBERS -
11. CONTROLLING OFFICE NAME AND ADDRESS Office of Naval Research Chemistry Program Office Arlington, VA 22217		12. REPORT DATE January, 1980 13. NUMBER OF PAGES
14. MONITORING AGENCY NAME & ADDRESS(if different from Controlling Office)		15. SECURITY CLASS. (of this report) Unclassified 15a. DECLASSIFICATION/DOWNGRADING SCHEDULE

16. DISTRIBUTION STATEMENT (of this Report)

Approved for Public Release; Distribution Unlimited.

17. DISTRIBUTION STATEMENT (of the abstract entered in Block 20, if different from Report)

18. SUPPLEMENTARY NOTES

Preprint: to be published in the J. Chem. Physics

19. KEY WORDS (Continue on reverse side if necessary and identify by block number)

Chemisorption, nuclear magnetic resonance, ^{13}C, carbon monoxide, rhodium, catalysis, spin-lattice relaxation times, infrared intensities, site exchange.

20. ABSTRACT (Continue on reverse side if necessary and identify by block number)

The ^{13}C NMR spectrum of carbon monoxide chemisorbed on supported rhodium has been studied. Lineshapes for two forms of chemisorbed carbon monoxide have been separated based on differences in spin-lattice relaxation times. These data have been used to estimate the molar integrated intensities for the infrared spectrum of various chemisorbed species reported previously.

DD FORM 1 JAN 73 1473 EDITION OF 1 NOV 65 IS OBSOLETE
S/N 0102-014-6601 |

UNCLASSIFIED

SECURITY CLASSIFICATION OF THIS PAGE (When Data Entered)